Available online at www.sciencedirect.com
SCIENCE DIRECT
Journal of Solid State Chemistry 179 (2006) 1630–1635
JOURNAL OF SOLID STATE CHEMISTRY
www.elsevier.com/locate/jssc

Formation and stability of Gd, Y, Yb and Lu disilicates and their solid solutions

N. Maier[a], G. Rixecker[b,1], K.G. Nickel[a,*]

[a]Eberhard-Karls-University Tuebingen, Applied Mineralogy, Wilhelmstr. 56, D-72074 Tuebingen, Germany
[b]Max-Planck-Institute for Metals Research, Heisenbergstr. 3, D-70569 Stuttgart, Germany

Received 13 October 2005; received in revised form 30 January 2006; accepted 15 February 2006
Available online 6 March 2006

Abstract

The synthesis and the phase stability regions of the disilicates of Y, Lu, Yb and Gd have been investigated at temperatures between 1300 and 1600 °C. The mean ionic radius of the rare-earth element ion including Y turns out to be the key parameter to govern the stabilities of polymorph types of both pure disilicates and their solid solutions. Both are predicted correctly by the phase stability diagram of Felsche [1] [J. Felsche, Struct. Bond. 13 (1973) 99–197]. Furthermore, it correlates with the reactivity, with increasing radius a faster reaction is observed at a given temperature. A fast reactivity is assumed to create difficulties in the densification of disilicates with ionic radius exceeding ~0.88 Å. In the reaction from oxide powders monosilicates are formed in a first step. Disilicates are formed from those initially in the form of low-temperature modifications, which transform in a sequence to high-temperature modifications.

Keywords: Rare-earth elements; Silicates; Phase diagram; Reactivity; Formation

1. Introduction

Rare-earth disilicates $RE_2Si_2O_7$ (RE = rare earth element, including Y) have been studied during the past decades with different motivations. First they were studied because of their unique magnetic, electrical and optical properties, making them interesting materials for e.g. the application in microwave technology, ferromagnetics, lasers and phosphors [1,2]. More recently, the interest in these materials has been renewed because they are products of sintering or corrosion of Si_3N_4 or SiC ceramics containing rare-earth oxides as sintering additives [3–7]. Additionally, several rare-earth disilicates are currently studied for the possible use as environmental barrier coatings for the protection of structural ceramics in severely corrosive environments [6–12].

The data presented here come from a study on the latter application. The silicates were manufactured to be used as homogeneous and dense samples for corrosion tests described elsewhere [13,14]. For this reason the compositions chosen and sintering conditions used do not follow the systematics of usual phase relation studies.

It is long known that many rare-earth disilicates show polymorphism as recently summarized in [15]. For those containing rare-earth elements (REE) with an ionic radius equal to or smaller than Y the four high-temperature polytypes α, β, γ and δ (also referred to as B, C, D and E, respectively [1]) are known at normal pressure [16–18] and additional structures at elevated pressure [15]. For $Y_2Si_2O_7$, other low-temperature phases (y and z) were reported, which are probably stabilized by impurities [2,18–22].

The phase relationships of the different polytypes of $Y_2Si_2O_7$ were extensively studied by Ito and Johnson [16] in the late 1960s. For the four high-temperature phases of this silicate, α, β, γ and δ, they found the following, transformation temperatures:

$$\alpha \rightarrow 1225\,^{\circ}C \rightarrow \beta \rightarrow 1445\,^{\circ}C \rightarrow \gamma \rightarrow 1535\,^{\circ}C \rightarrow \delta.$$

However, some recent studies seem to be in contradiction to these findings. For example, studies of Parmentier et al.

*Corresponding author. Fax: +49 70 71 29 30 60.
E-mail address: klaus.nickel@uni-tuebingen.de (K.G. Nickel).
[1]Robert Bosch GmbH, CR/ART2, Postfach 10 60 50, D-70049 Stuttgart, Germany.

0022-4596/$ - see front matter © 2006 Elsevier Inc. All rights reserved.
doi:10.1016/j.jssc.2006.02.019

[18] or Becerro et al. [20] indicated that the γ phase already forms at temperatures of 1350 °C or below. Additionally, the authors of [18] did not succeed in sintering the δ phase at 1600 °C. An yttrium silicate sintered by Fukuda and Matsubara [23] at 1600 °C and subsequently quenched in air similarly showed γ phase, not the δ phase expected from the predictions of Ito and Johnson [16] (the $Y_2Si_2O_7$ in [23] is referred to as δ phase, the structural parameters determined by the authors prove however, that in fact γ phase was synthesised). This problem will be addressed in this paper considering experimental results and literature reports.

Parmentier et al. [18] found evidence that during reaction sintering of oxides, α-$Y_2Si_2O_7$ is formed as a primary reaction product (independent of sintering temperature) which is transformed successively into the polytype stable at the actual sintering temperature along the path $\alpha \rightarrow \beta \rightarrow \gamma$ ($\rightarrow \delta$?).

Other authors found different initial products and transformation paths for different educts [4,20–22]. We revisit this problem in the light of new experimental findings.

Solid solubility between disilicates of different REE has been reported [16,24–26]. There is clear evidence that the incorporation of REE of one type into the disilicate of a REE of another type has a strong influence on the stability of the structure types of the silicate at normal pressure [24–27]. Up to now, however, information on the nature and extent of this influence is scarce. Our study provides additional information for a better understanding of the phase stabilities in solid solutions of rare earth disilicates.

2. Experimental

All materials were reaction sintered from oxide powder mixtures. As starting materials, powders of SiO_2 (CERAC, 99.9% purity), Gd_2O_3 (ALFA AESAR, 99.99% purity), Y_2O_3 (H. C. STARCK, 99.9% purity), Yb_2O_3 (CHEMPUR, 99.99% purity) and Lu_2O_3 (ABCR, 99.9% purity) were used. Powder mixtures were milled in an attritor mill for 3 h in isopropanol to yield oxide mixtures with fine grain sizes ($D_{50} < 1$ μm). Si_3N_4 balls were used as grinding media. Dried powder mixtures were cold isostatically pressed into cylinders of approximately 1–6 cm height and 0.6–0.8 cm radius. These green bodies were sintered in covered platinum crucibles using NABERTHERM chamber kilns.

The abbreviations for the powder mixtures as used in this paper are listed in Table 1 and the sintering treatments of the mixtures are listed in Table 2. Unless stated in Table 2 the heating and cooling rates in the sintering experiments were in the range of 2–10 °C/min.

In samples marked "#" in Table 2, no complete homogenization of the oxide powders was achieved prior to sintering due to segregation effects in the powder suspensions. These occurred when the powders were not dried directly after milling, especially when the powder suspensions were highly disperse and allowed differential settling of powder components. Reaction of the oxides to disilicate was nearly complete nonetheless. We assume that the trace amounts of monosilicate and unreacted silica present in the samples do not influence the phase stabilities discussed in this paper, as it was done in earlier studies where minor amounts of secondary phases were present after disilicate synthesis [18,26].

Table 1
Powder mixtures

Stoichiometry (molar ratio)	Sample designation
$1Y_2O_3{:}2SiO_2$	Y
$1Yb_2O_3{:}2SiO_2$	Yb
$1Lu_2O_3{:}2SiO_2$	Lu
$0.75Y_2O_3{:}0.25Gd_2O_3{:}2SiO_2$	75YGd
$0.75Y_2O_3{:}0.25Yb_2O_3{:}2SiO_2$	75YYb
$0.75Y_2O_3{:}0.25Lu_2O_3{:}2SiO_2$	75YLu
$0.5Y_2O_3{:}0.5Yb_2O_3{:}2SiO_2$	50YYb
$0.5Y_2O_3{:}0.5Lu_2O_3{:}2SiO_2$	50YLu

XRD measurements (PHILLIPS PW1050, Cu$K\alpha$ radiation and BRUKER D8 GADDS, Co$K\alpha$ radiation) on ground pieces of the sintered samples were conducted to determine the phase content. Porosity, phase distribution and in some cases phase composition was checked by scanning electron microscopy (SEM) and EDX using ZEISS DSM 962, DSM 982 Gemini, JEOL JXA 8900 and JSM 6400.

Densities were determined by dividing the weight of the samples by their volumes assessed by measurements with a sliding calliper.

3. Results

Phases detected by XRD and/or EDX examinations are given in Table 2.

EDX confirmed the elemental ratios of the powder mixes in the disilicates (some positive and negative deviations from the ideal Y-REE ratios in single grains occurred in incompletely homogenized samples), indicating complete solid solubility for all stoichiometries investigated. XRD shows only reflexes of a single disilicate phase in all cases. For the mixed silicates, most peaks are shifted towards larger 2Θ-angles compared to pure Y disilicate in the respective modification (except 75YGd with a shift towards smaller angles) as visible from Fig. 1; some peak intensities also change. This is in accordance with findings by Becerro and Escudero [26] for mixtures of $Y_2Si_2O_7$ and $Lu_2Si_2O_7$.

Semiquantitative Rietveld-like analysis using SIROQUANT (Sietronics Pvt Ltd) on 50YYb and 50YLu showed that the lattice constants a_0 and b_0 of the solid solutions in a given structure type are approximately the concentration-related average values of the lattice constants of the pure end member silicates in the β-modification [13] as was also reported in [26]. The value of c_0 is nearly the same for all three end member silicates, so no

Table 2
Sintering treatments and phases detected

Sample designation	Run	Sintering temperature/time	Post-sintering treatment	Remarks	Phases detected
Y	1	1320 °C/48 h			Disilicate (γ) Disilicate (β) (weak)
	2	1350 °C/no dwell time		*	Monosilicate Silica Disilicate (β) Disilicate (α) (weak)
	3	1400 °C/24 h		#	Disilicate (β) Disilicate (γ) (weak) Monosilicate (weak) Silica (weak)
	4	1400 °C/24 h	1370 °C/24 h	#	Disilicate (β) Disilicate (γ) Monosilicate (weak) Silica (weak)
	5	1400 °C/20 h	1600 °C/2.5 h		Disilicate (γ)
	6	1600 °C/5 h			Disilicate (γ)
	7	1600 °C/8 h		Air quench; #	Disilicate (γ) Silica (weak)
Yb	1	1600 °C/5 h			Disilicate (β)
Lu	1	1350 °C/no dwell time		Same treatment as Y-2; *	Monosilicate Silica Disilicate (β)
	2	1600 °C/5 h			Disilicate (β)
75YGd	1	1600 °C/6 h			Disilicate (δ)
75YYb	1	1400 °C/24 h	1500 °C/6 h	1400 °C to 1500 °C at 0.3 K/min	Disilicate (γ)
	2	1500 °C/10 h		#	Disilicate (β) Disilicate (γ) (weak) Monosilicate (weak) Silica (weak)
	3	1600 °C/5 h		#	Disilicate (β) Disilicate (γ) (weak) Monosilicate (weak) Silica (weak)
	4	1600 °C/15 h		#	Disilicate (γ) Silica (weak)
75YLu	1	1400 °C/24 h	1500 °C/1 h	1400 °C to 1500 °C at 0.3 K/min	Disilicate (β) Disilicate (γ)
	2	1400 °C/24 h	1500 °C/6 h		Disilicate (γ) Disilicate (β)
	3	1500 °C/20 h			Disilicate (γ)
50YYb	1	1350 °C/no dwell time		Same treatment as Y-2; *	Monosilicate Silica Disilicate (β) Disilicate (α) (weak)
	2	1525 °C/16 h			Disilicate (β)
50YLu	1	1500 °C/20 h			Disilicate (β)

= incomplete homogenization.
* = homogenous samples with incomplete reaction: small amounts of rare-earth oxide might be present; a definite identification by XRD is impossible because of peak overlap.

clear change is visible. Accordingly, no shift of the (001)-peak of 50YYb at approximately 22.3° is visible in Fig. 1. 75YYb and 75YLu also show lattice constants a_0 and b_0 which are smaller than those of pure γ-$Y_2Si_2O_7$ [13].

The coexistence of disilicate with minor amounts of monosilicate and silica (the latter only detectable by EDX) in samples marked # in Table 2 is attributed to segregation effects during powder preparation as mentioned above.

In all well-homogenized samples monosilicate is very rare and only detectable in SEM; silica could not be detected but might be present in small amounts on grain boundaries. Large amounts of monosilicate and silica in

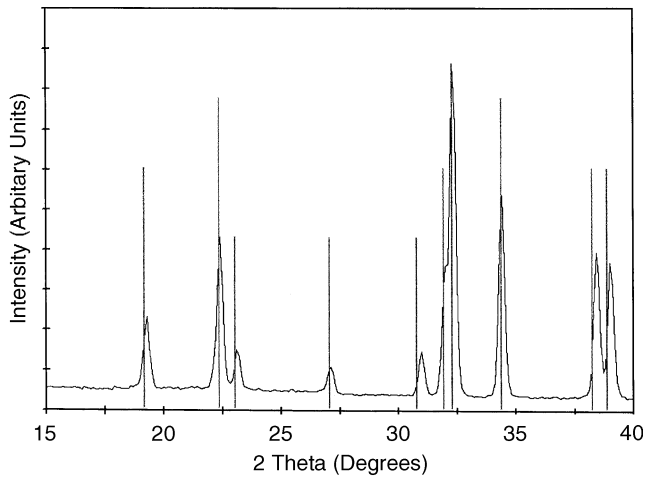

Fig. 1. Peak shifts in 50YYb-2 compared to pure yttrium disilicate; vertical lines mark the peak positions of β-$Y_2Si_2O_7$ (PDF 380440).

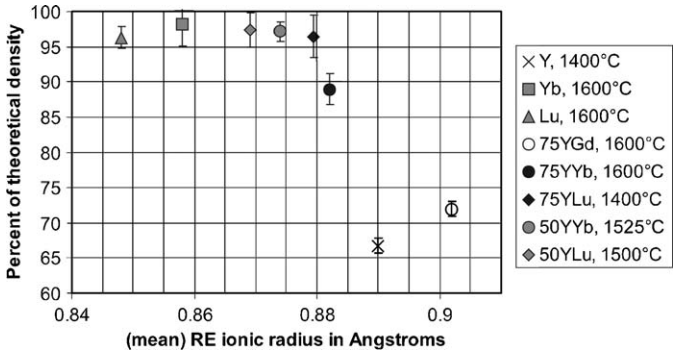

Fig. 2. Relative densities of silicates produced.

samples Y-2, Lu-1 and 50YYb-1 are attributed to low sintering temperatures and short sintering times which did not allow complete reaction.

Only samples with mean rare-earth ionic radii smaller than ~0.88 Å could be densified to >95% of the theoretical values (Fig. 2). The theoretical densities of solid solutions were approximated as mean values of the densities of the end members. No significant changes in sintering densities were observed for different sintering temperatures in measurements on materials Y and 75YLu [13].

4. Discussion

The well-homogenized samples with incomplete reactions (Y-2, Lu-1 and 50YYb-1) can be used to assess reaction rates for silicate formation in these systems.

Judging from XRD peak intensity ratios from short-time experiments at 1350 °C, sample Y-2 has clearly higher ratios of disilicate to monosilicate than 50YYb-1, which again shows higher ratios than Lu-1. Thus the rate of formation of disilicate seems faster in yttrium-rich compositions compared to those enriched in smaller REE.

This may also explain the problem of obtaining dense disilicates with large ionic radius. The volume losses during the reaction of oxides to disilicates exceed 10% for all sintered compositions. A fast reaction might thus create porosity faster than it can be reduced by sintering and promotes pore entrapment in grains. Higher temperatures only cause coarsening rather then densification.

The presence of very large amounts of monosilicate together with disilicate in incompletely reacted samples Y-2, Lu-1 and 50YYb-1 indicates that disilicates are not formed directly. The first step is the monosilicate formation:

$$RE_2O_3 + SiO_2 \rightarrow RE_2SiO_5 \quad (1)$$

from which disilicates are formed by the reaction

$$RE_2SiO_5 + SiO_2 \rightarrow RE_2Si_2O_7 \quad (2)$$

The disilicates are not formed as the equilibrium modification. Comparing runs Y-3 and Y-4 we have evidence for a formation of β-$RE_2Si_2O_7$ before it is transformed slowly to the γ-phase. The same is true for 75YYb at 1600° (runs 75YYb-3 and 75YYb-4). In short runs, the low-temperature trace amounts of the low-temperature modification α are observed together with β phase (runs Y-2 and 50YYb-1).

This supports the findings of Parmentier et al. [18], who suggested a standard path for high-temperature modifications in $Y_2Si_2O_7$ to form in a succession starting with the low-temperature polymorph α. According to our results this successive transformation occurs also in other rare-earth disilicates. This is also backed by findings of Becerro and Escudero [25] for solid solutions of Lu and Y disilicates, where low- and high-temperature polytypes coexist after sintering at low temperatures. The initial formation of α phase in our experiments cannot be explained by a crystallization process from an amorphous state as suggested [18]. In fact, a preferred formation of δ, γ or β phase of $Y_2Si_2O_7$ in melt crystallization experiments has been reported [4]. This indicates that structural features of crystallising melts indeed promote the formation of high-temperature polytypes (at least in pure disilicate melts; in the presence of aluminium, y phase has also been reported [21]) while during reaction sintering of oxides, low-temperature forms seem to form preferably. The initial polymorph formed is α in several cases reported [18,19], as it was found in our study; the initial formation of the polytype y in some sol–gel processes [18,19,25] might be due to stabilising effects of water from the precursor as suspected by Kepinski and Wolcyrz [19] and might also be connected with a crystallization process from an amorphous state.

The preferred formation of low-temperature phase α might be explained by the two-step formation of disilicate via monosilicate which was described above. There are structural similarities between monosilicate and α-disilicate. Monosilicate contains chain structures of oxygen coordinated by rare-earth ions and α-disilicate contains chains of rare-earth ions coordinated by oxygen [1,17]. Additionally, both structures contain isolated SiO_4

tetrahedra, while other disilicate polymorphs contain Si_2O_7 units [1]. These structural similarities should make an initial formation of α-phase during reaction (2) energetically favourable.

At least in the presence of [16,20] impurities the formation of the α polytype may be preceded by the formation of a *y*-type silicate. If this *y* polymorph transforms very rapidly into α we may have missed to observe it. However, there is no evidence for this from our experiments.

The absence of α-disilicate in Lu-1 may be due to the fact that that this polymorph does not exist in the Lu–Si–O system, even at temperatures below those examined before [1,16]. Alternatively, the phase might not have been detected after run Lu-1 because a relatively fast transformation $\alpha \rightarrow \beta$ phase (i.e. a reduced metastable preservation at the temperature tested) yielded contents of α-$Lu_2Si_2O_7$ below the detection limit in Lu-1.

The formation along transformations from low- to high-temperature modifications contrasts with reports of the direct formation of δ-, γ- or β-$Y_2Si_2O_7$ in melt crystallization experiments [4]. It is not unlikely that the structures of high-temperature melts include building blocks, which are akin to high-temperature crystalline structures. Accordingly, the preferred formation of *y*-$Y_2Si_2O_7$ from Saponite (both containing similar structural features) has been reported [20]. This may be the reason for strongly differing evolutions during solid-state synthesis compared to melt synthesis methods. Additionally, comparing [4] and [21], glass composition and the presence of impurities in a glass seem to have a clear influence on the crystallization and stability of different polytypes of yttrium disilicate.

Our results on the stability of $Y_2Si_2O_7$ polymorphs contradict the widely used values of Ito and Johnson [16]. The latter predicted a phase transformation $\beta \rightarrow \gamma$ at 1445 °C and a transformation $\gamma \rightarrow \delta$ at 1535 °C. In our experiments, γ phase was stable even at the lowest tested sintering temperature of 1320 °C, so the phase boundary between β and γ must lie below that temperature. This is in agreement with more recent work [18,20] which report a transformation $\beta \rightarrow \gamma$ at temperatures of 1350 °C or below. Due to the fact that in [18] no γ phase was found after 24 h of sintering at 1300 °C, we presume the boundary to lie between 1300 and 1320 °C.

δ-$Y_2Si_2O_7$ could never be synthesized in our experiments at a temperature of 1600 °C, not even with a relatively long sintering time of 8 h and a subsequent quench of the sample in air (run Y-7). Together with other findings from the literature, which were discussed in the introduction of this paper, this indicates that a transformation $\gamma \rightarrow \delta$ is not occurring at 1535 °C [16] or another temperature $\leqslant$1600 °C. Neither a very slow formation of the δ phase from the γ modification nor a very fast transformation into this structure during cooling is a probable explanation for the nonexistence of δ-$Y_2Si_2O_7$ at 1600 °C, because nearly pure δ-disilicate is obtained at 1700 °C with only 2 h sintering time without subsequent quenching [18].

The differences to the studies on δ-$Y_2Si_2O_7$ at 1600 °C or below [4,16] may be resolved by the presence of impurities or additional (glassy?) phases, which potentially stabilize the δ phase at lower temperatures. A stabilization of a structure type of $(Y_{2/3}La_{1/3})_2Si_2O_7$ in the presence of a silica surplus has been reported [28]. In earlier experiments [13] we found δ-$Y_2Si_2O_7$ in insufficiently homogenized sintered powder mixtures, which yielded phase assemblages containing disilicates with considerable amounts of unreacted silica, monosilicate and yttrium oxide after treatment at 1600 °C.

Our data show that sintered oxide powders with mixed rare-earth oxides also form disilicates in the known structures α, β, γ and δ. However, from Table 2 it can be seen that solid solutions of Y with Gd, Yb and Lu in disilicates can stabilize modifications, which do not occur in pure end members at the given temperatures. The addition of 25 mol% $Gd_2Si_2O_7$ to yttrium disilicate leads to the formation of the δ structure at 1600 °C. The addition of 50 mol% Yb or Lu disilicate yields a product in the β modification at 1500 °C or higher. A similar stabilization of β-$RE_2Si_2O_7$ in mixtures of Lu and Y disilicates has recently been reported [25].

In a recent discussion of phase stabilities of rare-earth disilicate solid solutions, which was based on observations on Y–La disilicate solid solutions [27], it was suggested that the phase stabilities of a solid solution behave just like the phase stabilities of a silicate with RE ionic radius equal to the average of the radii of the rare earths in the solid solution. Mean ionic radii are calculated as

$$r_{RE}^{\text{mean}} = \sum \left(r_{RE_i} \frac{c_{RE_i}}{\sum_1^n c_{RE}} \right), \tag{3}$$

where r_{RE} and c_{RE} refer to ionic radius and molar concentration of the REE. The radius of 0.89 Å for Y^{3+} was adopted from [2,27].

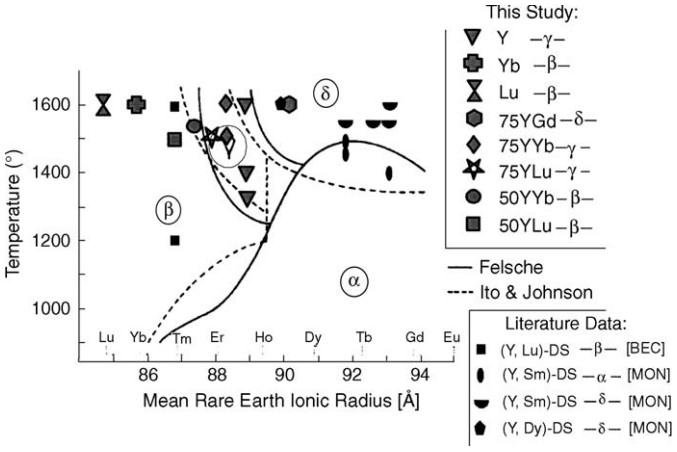

Fig. 3. Observed stable disilicate phases compared to phase stability predictions by Felsche [1] and Ito and Johnson [16] in a plot after Lidell and Thompson [2]. BEC = [25], MON = [24]. It is assumed that the stoichiometry of the solid solutions [24] is equal to the stoichiometry of the powder mixtures sintered by the authors. The silicates in [24] were synthesized in the presence of a large silica surplus.

In Fig. 3, all experimentally determined low-pressure phase stabilities are plotted against phase stability diagrams of Felsche [1] and Ito and Johnson [16]. All polymorphs, including those of the solid solutions (plotted according to Eq. (3)), are in accordance with the diagram of Felsche [1]. The same is true for further data of solid solutions taken from contemporary literature [24,25]. Therefore a prediction of phase stabilities of solid solutions of rare-earth disilicates seems possible from the diagram if ionic radii according to Eq. (3) are assumed. The older phase stability data of Ito and Johnson [16] do not allow correct predictions in all cases.

At least for the transformations $\beta \rightarrow \gamma \rightarrow \delta$, the diagram of Felsche [1] also seems to predict the stabilities of $Y_2Si_2O_7$ better than the boundaries suggested in [16] if the silicate is included in the diagram at its ionic radius of 0.89 Å (although the transformation $\beta \rightarrow \gamma$ suspected between 1300 and 1320 °C is not exactly predicted this way).

5. Conclusions

Disilicate solid solutions of Y with Lu, Yb and Gd can be treated as having a simple mean rare-earth ionic radius according to the relative content of end members. Our data show that the stability regions of the solid solutions of REE and Y are then well predicted by the phase stability diagram of Felsche [1], which should be preferred to that of Ito and Johnson [16].

As far as our data can tell, the mean ionic radius of the rare-earth element correlates also with the reactivity; for lower radii, slower reactions from oxides to disilicate were observed. The fast reactivity is assumed to create difficulties in the densification of disilicates with ionic radius exceeding ~0.88 Å.

The reaction from oxide powders to the equilibrium polymorph has several steps: Firstly monosilicates are formed, which continue to react to disilicates. Those are formed first in the form of low-temperature modifications, which transform in a sequence to high-temperature modifications.

Acknowledgments

We acknowledge the help in preparation of samples by U. Heinrichs and M. Schweizer of the Max-Planck-Institute for metals research in Stuttgart (MPI) and in the analysis and characterisation of samples by C. Berthold, E. Nadler and T. Wenzel of University Tübingen and H. Labitzke, F. Predel and C. Hofer from MPI.

References

[1] J. Felsche, Struct. Bond. 13 (1973) 99–197.
[2] K. Liddell, D.P. Thompson, Br. Ceram. Trans. 85 (1986) 17–22.
[3] M.K. Cinibulk, G. Thomas, J. Am. Ceram. Soc. 75 (8) (1992) 2044–2049.
[4] S. Kumar, C.H. Drummond, J. Mater. Res. 7 (4) (1992) 997–1003.
[5] H. Klemm, J. Eur. Ceram. Soc. 22 (2002) 2735–2740.
[6] K. A. Weidenmann, G. Rixecker, F. Aldinger, J. Eur. Ceram. Soc., in press.
[7] K.N. Lee, D.S. Fox, N.P. Bansal, J. Eur. Ceram. Soc. 25 (2005) 1705–1715.
[8] M. Aparicio, A. Duran, J. Am. Ceram. Soc. 83 (6) (2000) 1351–1355.
[9] T. Laux, T. Ullmann, M. Auweter-Kurtz, A. Kurz, in: Investigations of thermal protection materials along an X-38 reentry trajectory by plasma wind tunnel simulations, Second International Symposium on Atmospheric Reentry Vehicles and Systems, Arcachon (France), 2001; Arcachon (France), 2001, pp. 1–9.
[10] H. Klemm, M. Fritsch, B. Schenk, unpublished (2004) 6.
[11] I. Yuri, T. Hisamatsu, Proceedings of ASME TURBO EXPO, Atlanta, Georgia, 2003, pp. 1–9.
[12] T. Suetsuna, T. Ohji, J. Am. Ceram. Soc. 88 (5) (2005) 1139–1144.
[13] N. Maier, Synthese von Seltenerd-Disilikaten und deren Korrosionsverhalten an strömender feuchter Atmosphäre. Diploma Thesis, Eberhardt-Karls-Universität, Tübingen, 2005.
[14] N. Maier, K.G. Nickel, in: Influence of impurities on the high-temperature water-vapor corrosion of environmental barrier rare-earth silicates, Fourth China International Conference on High-Performance Ceramics, Chengdu (China), 23-26-10.2005, submitted for publication.
[15] M.E. Fleet, X. Liu, J. Solid State Chem. 178 (2005) 3275–3283.
[16] J. Ito, H. Johnson, The American Mineralogist 53 (Nov-Dec-Issue) (1968) 1940–1952.
[17] J. Felsche, in: Handbook of Geochemistry, vol. II/5, Springer, Heidelberg, 1978, p. 39 57-71-A-1 to 39, 57-71-A-42.
[18] J. Parmentier, P.R. Bodart, L. Audoin, G. Massouras, D.P. Thompson, R.K. Harris, P. Goursat, J.-L. Besson, J. Solid State Chem. 149 (2000) 16–20.
[19] L. Kepinski, M. Wolcyrz, Mater. Chem. Phys. 81 (2003) 396–400.
[20] A.I. Becerro, M. Naranjo, M.D. Alba, J.M. Trillo, J. Mater. Chem. 13 (2003) 1835–1842.
[21] T.R. Dinger, R.S. Rai, G. Thomas, J. Am. Ceram. Soc. 71 (4) (1988) 236–244.
[22] A.I. Becerro, M. Naranjo, A.C. Perdigón, J.M. Trillo, J. Am. Ceram. Soc. 86 (9) (2003) 1592–1594.
[23] K. Fukuda, H. Matsubara, J. Am. Ceram. Soc. 87 (1) (2004) 89–92.
[24] F. Monteverde, G. Celotti, J. Eur. Ceram. Soc. 22 (2002) 721–730.
[25] A.I. Becerro, A. Escudero, Chem. Mater. 17 (2005) 112–117.
[26] A.I. Becerro, A. Escudero, J. Solid State Chem. 178 (2005) 1–7.
[27] M.J. Pomeroy, E. Nestor, R. Ramesh, S. Hampshire, J. Am. Ceram. Soc. 88 (4) (2005) 875–881.
[28] F. Monteverde, G. Celotti, J. Eur. Ceram. Soc. 19 (1999) 2021–2026.